J. Fluid Mech. (2005), *vol.* 523, *pp.* 251–260.
DOI: 10.1017/S0022112004002289 Printed in the United Kingdom

Heat transport by turbulent Rayleigh–Bénard convection in cylindrical cells with aspect ratio one and less

By ALEXEI NIKOLAENKO, ERIC BROWN, DENIS FUNFSCHILLING AND GUENTER AHLERS

Department of Physics and iQUEST, University of California, Santa Barbara, CA 93106, USA

(Received 4 September 2004 and in revised form 8 October 2004)

We present high-precision measurements of the Nusselt number $\mathcal{N}$ as a function of the Rayleigh number R for cylindrical samples of water (Prandtl number $\sigma = 4.4$) with a diameter D of 49.7 cm and heights $L = 116.3$, 74.6, and 50.6 cm, as well as for $D = 24.8$ cm and $L = 90.2$ cm. For each aspect ratio $\Gamma \equiv D/L = 0.28$, 0.43, 0.67, and 0.98 the data cover a range of a little over a decade of R. The maximum $R \simeq 10^{12}$ and Nusselt number $\mathcal{N} \simeq 600$ were reached for $\Gamma = 0.43$ and $D = 49.7$. The data were corrected for the influence of the finite conductivity of the top and bottom plates on the heat transport in the fluid to obtain estimates of $\mathcal{N}_\infty$ for plates with infinite conductivity. The results for $\mathcal{N}_\infty$ and $\Gamma \geqslant 0.43$ are nearly independent of Γ. For $\Gamma = 0.275$ $\mathcal{N}_\infty$ falls about 2.5% below the other data. For $R \lesssim 10^{11}$, the effective exponent γ_{eff} of $\mathcal{N}_\infty = N_0 R^{\gamma_{eff}}$ is about 0.32, larger than those of the Grossmann–Lohse model with its current parameters by about 0.01. For the largest Rayleigh numbers covered for $\Gamma = 0.98$, 0.67, and 0.43, γ_{eff} saturates at the asymptotic value $\gamma = 1/3$ of the Grossmann–Lohse model. The data do not reveal any crossover to a Kraichnan regime with $\gamma_{eff} > 1/3$.

1. Introduction

Understanding turbulent Rayleigh–Bénard convection (RBC) in a fluid heated from below (e.g. Siggia 1994; Kadanoff 2001; Ahlers, Grossmann & Lohse 2002) is one of the challenging and largely unsolved problems in nonlinear physics. An important aspect is the global heat transport that is usually expressed in terms of the Nusselt number

$$\mathcal{N} = QL/\lambda\Delta T. \tag{1.1}$$

Here Q is the heat-current density, L the sample height, ΔT the applied temperature difference, and λ the thermal conductivity of the fluid in the absence of convection. A central prediction of various theoretical models (Kraichnan 1962; Siggia 1994; Grossmann & Lohse 2000, 2001, 2002, 2004) is a relationship between $\mathcal{N}$, the Rayleigh number $R = \alpha g \Delta T L^3/\kappa\nu$ (α is the isobaric thermal expension coefficient, κ the thermal diffusivity, ν the kinematic viscosity, and g the acceleration of gravity), and the Prandtl number $\sigma = \nu/\kappa$. A model developed recently by Grossmann & Lohse (2000), based on the decomposition of the kinetic and the thermal dissipation into boundary-layer and bulk contributions, provided an excellent fit to experimental data of Xu, Bajaj & Ahlers (2000) and Ahlers & Xu (2001) for a cylindrical cell of aspect ratio $\Gamma \equiv D/L = 1$ (D is the sample diameter) when it was properly adapted

(Grossmann & Lohse 2001, referred to hereafter as GL) to the relatively small Reynolds numbers of the measurements. However, the data were used to determine five adjustable parameters of the model. Thus more stringent tests using measurements for the same Γ but over wider ranges of R and σ are desirable. A great success of the model was the excellent agreement with recent results by Xia, Lam & Zhou (2002) for much larger Prandtl numbers than those of Ahlers & Xu (2001), at Rayleigh numbers near 1.78×10^7 and 1.78×10^9.

Here we present new measurements in a cell of diameter $D = 49.7\,\mathrm{cm}$ for $\sigma \simeq 4.4$ that, for $\Gamma = 0.98$, extend to $R \simeq 10^{11}$. We also report results for $D = 49.7\,\mathrm{cm}$ and $\Gamma = 0.427$ and 0.667, as well as for $D = 24.8\,\mathrm{cm}$ and $\Gamma = 0.275$. For $\Gamma \gtrsim 0.5$ it is expected that the large-scale flow (LSF) in the cell (Krishnamurty & Howard 1981) consists of a single convection roll (Verzicco & Camussi 2003). For $\Gamma \lesssim 0.5$, on the other hand, Verzicco & Camussi (2003) suggest that the system contains two or more rolls placed vertically one above the other. How this affects the heat transport was one of the questions to be addressed here. Work by Roche *et al.* (2004) had suggested a reduced heat transport for the two-roll structure. Based on this result, our measurements suggest that even the cell with $\Gamma = 0.43$ still contained only one roll because the data for $\mathcal{N}$ fall on the smooth line drawn through those for the larger Γ. The $\Gamma = 0.28$ results fall about 2.5% below all the other data, suggesting a more complicated, perhaps two-roll, structure for the LSF.

Most of our measurements were made at a mean temperature of 40 °C, where $\sigma = 4.38$, $\kappa = 6.7\,\mathrm{cm^2\,s^{-1}}$, $\alpha = 0.000388\,\mathrm{K^{-1}}$, $\lambda = 0.0063\,\mathrm{W\,cm^{-1}\,K}$. However, for $\Gamma = 0.67$ we also made measurements at mean temperatures of 50 °C and 30 °C, corresponding to $\sigma = 3.62$ and 5.42 respectively. We found a very gentle decrease of $\mathcal{N}$ with increasing σ, approximately in proportion to $\sigma^{-0.044}$. All of our measurements are expected to conform closely to the Boussinesq approximation. For the largest $\Delta T \simeq 20\,^\circ\mathrm{C}$ we have $\alpha \Delta T = 0.008$ and the ratio of the temperature drop across the top and bottom boundary layer is estimated to be $x_{WL} = 1.15$.

One of the experimental problems in the measurement of $\mathcal{N}(R)$ is that the sidewall often carries a significant part of the heat current. Corrections for this effect are not easily made, because of the thermal contact between the wall and the fluid that yields a two-dimensional temperature field in the wall, and because of the influence of lateral heat currrents through the wall on the fluid flow (Ahlers 2000; Roche *et al.* 2001; Verzicco 2002; Niemela & Sreenivasan 2003). The present project was designed to provide data that are not uncertain because of a significant sidewall correction. We used a classical fluid of relatively large conductivity confined by sidewalls of relatively low conductivity. The system of choice was water confined by Plexiglas with various heights L, and with the greatest diameter permitted by other constraints. We built four convection cells, three with $D = 49.67\,\mathrm{cm}$ with heights $L = 116.33$, 74.42, and 50.61 cm, and one with $D = 24.81\,\mathrm{cm}$ and $L = 90.18\,\mathrm{cm}$. For the $\Gamma = 0.98$ ($L = 50.61$) cell, which is most relevant to comparison with the theoretical model of GL, we estimated a wall correction (using Model 2 of Ahlers 2000) of only 0.3% for $R = 5 \times 10^9$ ($\mathcal{N} \simeq 100$) and smaller corrections for larger R. Based on this estimate we felt justified in neglecting the correction.

A second experimental problem was pointed out recently by Chaumat, Castaing & Chillá (2002) and Verzicco (2004). Using direct numerical simulation, Verzicco (2004) showed that end plates of finite conductivity diminish the heat transport in the fluid when the Nusselt number becomes large. In a separate paper we shall give details of the apparatus used in our work (Brown *et al.* 2005). There we will describe measurements using two types of top and bottom plates of identical shape and size,

No.	$\bar{T}$(°C)	ΔT(°C)	$10^{-8}R$	$\mathcal{N}$	$\mathcal{N}_\infty$	No.	$\bar{T}$(°C)	ΔT(°C)	$10^{-8}R$	$\mathcal{N}$	$\mathcal{N}_\infty$
1	39.932	2.122	576.8	229.1	229.5	2	39.964	4.036	1098.4	281.4	282.3
3	40.001	5.935	1617.2	317.2	318.6	4	40.044	7.817	2133.1	346.6	348.6
5	40.090	9.689	2648.5	371.1	373.6	6	40.141	11.553	3163.5	392.4	395.4
7	40.191	13.405	3677.1	411.4	415.0	8	39.997	2.983	812.7	255.1	255.7
9	40.032	4.888	1333.4	298.5	299.7	10	40.015	3.934	1072.6	278.6	279.4
11	40.012	2.261	616.4	233.7	234.1	12	39.990	6.448	1756.4	325.5	327.1
13	39.994	13.406	3652.1	410.0	413.6	14	39.973	8.941	2433.8	361.2	363.4
15	40.020	10.809	2947.2	383.3	386.1	16	39.998	11.833	3224.0	393.7	396.8
17	40.017	15.710	4283.1	430.5	434.7	18	40.007	13.773	3753.6	413.2	416.9
19	40.031	17.636	4810.5	446.6	451.3	20	40.002	19.647	5353.6	462.0	467.3
21	39.997	9.872	2689.6	372.2	374.7	22	39.997	7.908	2154.5	347.4	349.3

TABLE 1. Results for $\Gamma = 0.275$ and $D = 24.81$ cm. In this and all following data tables two points are listed in each row, and the points are numbered in chronological sequence.

No.	$\bar{T}$(°C)	ΔT(°C)	$10^{-8}R$	$\mathcal{N}$	$\mathcal{N}_\infty$	No.	$\bar{T}$(°C)	ΔT(°C)	$10^{-8}R$	$\mathcal{N}$	$\mathcal{N}_\infty$
1	39.849	19.921	11603.4	595.4	624.7	2	39.976	17.705	10358.7	574.5	601.6
3	40.021	15.661	9177.2	553.1	577.9	4	40.028	13.693	8025.7	529.2	551.7
5	39.993	11.811	6914.1	505.3	525.4	6	39.996	9.843	5763.1	476.9	494.6
7	40.092	7.689	4517.2	441.1	455.8	8	40.008	3.936	2305.5	356.1	364.8
9	40.009	1.965	1151.2	286.0	291.0	10	40.053	2.862	1679.0	322.4	329.2
11	40.057	4.824	2830.3	380.6	390.8	12	39.979	5.958	3486.2	405.8	417.8
13	40.014	1.464	857.9	260.2	264.1						

TABLE 2. Results for $\Gamma = 0.427$ and $D = 49.7$ cm.

but with one set made of copper with a conductivity $\lambda_{Cu} = 391\ \mathrm{W\,m^{-1}\,K}$ and the other of aluminium with $\lambda_{Al} = 161\ \mathrm{W\,m^{-1}\,K}$. That work yielded a correction factor that has been applied to the data reported here.

2. Results

2.1. *The measurements*

Details of the apparatus and of experimental procedures are given by Brown *et al.* (2005). The precision of the measurements is typically near 0.1%, and systematic errors, primarily due to uncertainties of the diameter and length of the cell, are estimated to be near 1%. Deviations from the Boussinesq approximation are believed to be unimportant (Brown *et al.* 2005). Measurements of the heat current with fixed top and bottom temperatures for time intervals of up to three days revealed no long transients; the system had always reached a stationary state after about two hours. We give the results in tables 1 to 4. The measured $\mathcal{N}$ derived from (1.1) as well as the Nusselt number $\mathcal{N}_\infty$ obtained after correction for the finite top- and bottom-plate conductivity (Verzicco 2004) are listed. The relation between these is given by $\mathcal{N} = f(X)\mathcal{N}_\infty$ where X is the ratio of the average thermal resistance of the plates to that of the fluid. We used the empirical function $f(X) = 1 - \exp[-(aX)^b]$, with the parameters $a = 0.275$ and $b = 0.390$ for $D = 49.7$, and $a = 0.304$ and $b = 0.506$ for $D = 24.82$, determined experimentally (Brown *et al.* 2005). The parameters were found to be independent of the aspect ratio but to depend on the plate diameter.

No.	$\bar{T}$(°C)	ΔT(°C)	$10^{-8}R$	$\mathcal{N}$	$\mathcal{N}_\infty$	No.	$\bar{T}$(°C)	ΔT(°C)	$10^{-8}R$	$\mathcal{N}$	$\mathcal{N}_\infty$
1	39.922	17.639	2693.9	371.5	389.3	2	39.816	16.035	2439.8	359.5	376.0
3	39.923	13.881	2120.1	343.9	358.8	4	39.937	11.892	1817.2	327.7	341.0
5	39.984	7.891	1207.7	288.0	297.9	6	39.995	3.955	605.5	231.5	237.3
7	40.013	1.952	299.1	185.8	189.1	8	39.979	19.633	3004.5	384.2	403.4
9	39.964	20.637	3156.4	389.9	409.7	10	39.898	18.821	2872.0	378.4	396.9
11	39.984	16.693	2555.0	365.1	382.2	12	39.915	14.875	2271.3	351.4	367.1
13	39.890	12.974	1979.2	336.5	350.6	14	40.109	10.574	1625.6	316.0	328.3
15	39.974	8.900	1361.7	299.4	310.2	16	40.059	2.846	436.8	209.0	213.5
17	39.974	17.693	2707.1	371.7	389.5	18	49.989	19.566	4101.7	426.0	450.1
19	49.886	18.789	3927.2	420.2	443.6	20	49.969	17.651	3698.0	412.3	434.8
21	49.959	5.003	1047.9	277.7	286.8	22	50.087	6.710	1410.6	304.8	316.0
23	50.136	8.576	1805.4	329.9	343.4	24	50.146	10.503	2211.6	351.2	366.8
25	50.174	12.406	2614.4	370.4	388.1	26	50.097	14.525	3054.1	388.4	408.1
27	49.902	4.140	865.7	261.6	269.4	28	49.935	3.092	647.1	239.0	245.3
29	49.928	2.120	443.6	212.4	217.0	30	49.973	1.046	219.1	172.3	175.0
31	39.974	17.693	2707.1	371.7	389.5	32	29.980	19.647	2007.0	336.1	350.3
33	29.996	17.656	1805.0	325.1	338.2	34	29.841	16.006	1624.5	314.4	326.6
35	29.742	14.246	1439.0	302.2	313.2	36	29.913	11.963	1218.2	287.0	296.8
37	29.957	9.918	1012.1	270.5	278.9	38	29.932	8.011	816.6	252.8	260.0
39	29.859	6.190	628.8	232.5	238.3	40	29.897	4.157	423.0	205.0	209.2
41	29.904	2.171	221.0	167.0	169.5	42	30.036	2.898	296.8	183.6	186.8
43	30.011	4.913	502.6	216.6	221.5	44	30.018	6.858	701.8	240.6	246.9
45	29.992	2.491	254.6	174.3	177.1						

TABLE 3. Results for $\Gamma = 0.667$ and $D = 49.7$ cm.

No.	$\bar{T}$(°C)	ΔT(°C)	$10^{-8}R$	$\mathcal{N}$	$\mathcal{N}_\infty$	No.	$\bar{T}$(°C)	ΔT(°C)	$10^{-8}R$	$\mathcal{N}$	$\mathcal{N}_\infty$
1	40.092	1.792	86.7	125.3	127.5	2	40.006	2.940	141.7	145.6	148.9
3	40.015	3.898	188.0	158.8	162.9	4	39.975	4.951	238.4	170.9	175.7
5	39.953	5.969	287.2	181.2	186.8	6	39.933	6.979	335.6	190.2	196.4
7	39.933	7.952	382.3	197.9	204.8	8	39.966	9.832	473.3	211.4	219.4
9	39.935	11.829	568.8	224.2	233.4	10	39.916	13.803	663.3	235.1	245.4
11	40.039	15.500	748.1	244.3	255.5	12	39.407	16.728	789.6	248.3	259.9
13	39.933	17.645	848.4	254.1	266.3	14	40.038	2.386	115.1	136.2	138.9
15	39.996	1.489	71.8	118.0	119.9	16	39.935	17.638	848.2	254.0	266.3
17	39.943	17.633	848.2	254.2	266.4						

TABLE 4. Results for $\Gamma = 0.981$ and $D = 49.7$ cm.

2.2. *Dependence on R and Γ*

The results for $\mathcal{N}_\infty$ are shown on logarithmic scales in figure 1(*a*) and with greater resolution in the compensated form $\mathcal{N}_\infty/R^{1/3}$ in figure 1(*b*). We note that over most of the range of R the data for $\Gamma \geqslant 0.43$ reveal very little if any dependence of $\mathcal{N}_\infty$ on Γ. Recent considerations by Grossmann & Lohse (2003) had suggested a stronger Γ-dependence. Earlier experimental data (Wu & Libchaber 1992; Xu *et al.* 2000) also suggested a stronger Γ dependence; but those results were influenced by sidewall and/or end-plate effects. Note for instance that the sidewall correction made by Ahlers (2000) considerably reduced the Γ dependence originally seen by Xu *et al.* 2000). Similarly, our present results for $\mathcal{N}$ reveal some dependence on Γ, but the end-plate correction largely removes it. It is particularly noteworthy that the data for $\Gamma = 0.43$ are not shifted significantly relative to those for $\Gamma = 0.67$ because on the basis of the numerical calculations of Verzicco & Camussi (2003) one expects

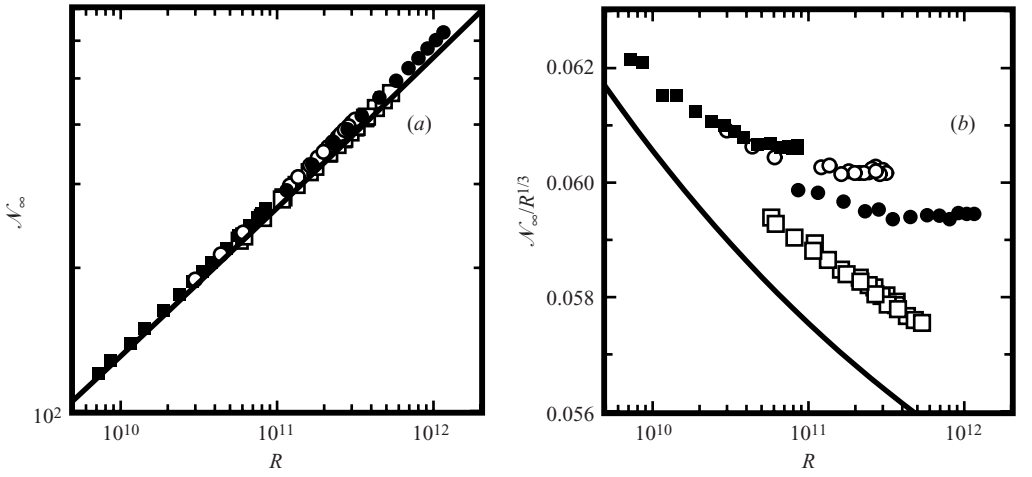

FIGURE 1. (*a*) The Nusselt number $\mathcal{N}_\infty$ as a function of the Rayeigh number R on logarithmic scales. (*b*) The compensated Nusselt number $\mathcal{N}_\infty/R^{1/3}$ as a function of the Rayleigh number R. Open squares: $\Gamma = 0.275$. Solid circles: $\Gamma = 0.43$. Open circles: $\Gamma = 0.67$. Solid squares: $\Gamma = 0.98$. Solid lines: the prediction of Grossmann & Lohse (2001) for $\sigma = 4.4$.

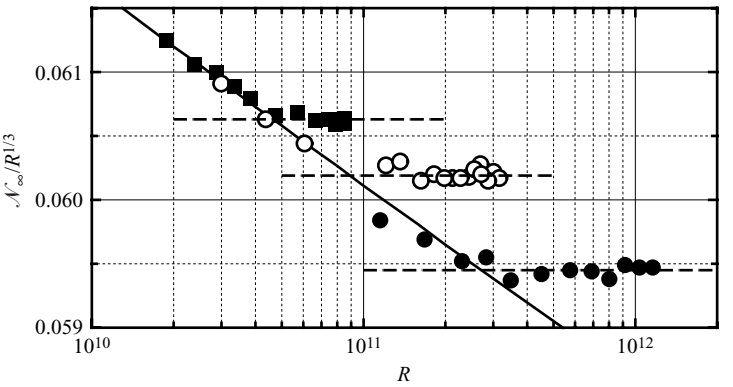

FIGURE 2. The compensated Nusselt numbers $\mathcal{N}_\infty/R^{1/3}$ as a function of the Rayleigh number R for $\Gamma = 0.98$ (solid squares), $\Gamma = 0.67$ (open circles), and $\Gamma = 0.43$ (solid circles) as in figure 1(*b*) but on an expanded scale. Lines: power laws $\mathcal{N}_\infty = N_0 R^{\gamma_{eff}}$. Solid line: $N_0 = 0.0797$, $\gamma_{eff} = 0.3222$. Dashed lines: $\gamma_{eff} = 1/3$ and (from top to bottom) $N_0 = 0.06063$, 0.06019, 0.05945.

different structures for the LSF for these two cases. The data for $\Gamma = 0.275$ are lower by about 2.5%, suggesting that a transition in the LSF structure may occur between $\Gamma = 0.43$ and 0.275.

A second important feature of the data is their dependence on R. Locally, over a limited range, the measurements can be fitted by the power law

$$\mathcal{N}_\infty = N_0 R^{\gamma_{eff}}. \tag{2.1}$$

For the effective exponent we found $\gamma_{eff} = 0.323$ for $\Gamma = 1$ near $R = 2 \times 10^{10}$ and $\gamma_{eff} = 0.329$ for $\Gamma = 0.67$ near $R = 10^{11}$. As shown in figure 2, a single fit to most of the data for $\Gamma = 0.98, 0.67$, and 0.43 yields $\gamma_{eff} = 0.322$. All these values are close to, but definitely less than, the asymptotic large-R prediction $\gamma = 1/3$ of the GL model.

However, they are larger by about 0.01 or 0.015 than the GL prediction for $\Gamma = 1$ at the same R. This can also be seen qualitatively from figure 1(b) where the GL prediction with its present parameter values is shown as a solid line. It remains to be seen whether the model parameters can be adjusted so as to reproduce this feature also.

Another interesting aspect noticeable in figure 1(b) is that for $\Gamma = 0.98$, 0.67, and 0.43 there is an apparent sudden change in the R-dependence of $\mathcal{N}_\infty$ at large R to a power law with $\gamma = 1/3$, i.e. with the asymptotic prediction of the GL model. This is illustrated more clearly in figure 2 which shows the relevant data with higher resolution. A change to a 1/3 power law was also reported by Niemela & Sreenivasan (2003) for $\Gamma = 1$ and $\sigma \simeq 0.8$, albeit at somewhat larger values of R, near $R \simeq 10^{13}$. It is difficult to see how the GL model can reproduce the rather sudden transition at finite R to its asymptotic exponent value. Rather, it seems likely that a new physical phenomenon not yet contained in the model will have to be invoked. The transition occurs for $\Gamma = 0.98$, 0.67, and 0.43 near $R = 5\times10^{10}$, 9×10^{10}, and 3×10^{11} respectively and is reflected in the observation that the data for larger R fall on horizontal lines in the figures. In this range the measurements suggest a weak dependence on Γ, with $N_0(\gamma_{eff} = 1/3) = 0.0606$, 0.0602, and 0.0595 for $\Gamma = 0.98$, 0.67, and 0.43 respectively. One interpretation of these results for N_0 is that the heat transport is diminished, albeit only very slightly, by a larger travel distance, and presumably a larger period, of the LSF. At smaller R an effective power law with $N_0 = 0.0797$, $\gamma_{eff} = 0.322$ (solid line in figure 2) fits the data at all three Γ values within their statistical uncertainty, showing that the results are essentially Γ independent. It is a surprise that the data for $\Gamma = 0.67$ and 0.43 do not differ more from each other because different structures for the LSF had been predicted for these two cases (Verzicco & Camussi 2003). The $\Gamma = 0.275$ results do indeed have a Nusselt number that is smaller by about 2% to 3%, suggesting that the transition in the flow structure occurred between $\Gamma = 0.43$ and 0.275. Those results do not show the saturation at large R with $\gamma_{eff} = 1/3$, and lead to $\gamma_{eff} = 0.321$ over their entire range.

2.3. *Dependence on the Prandtl number σ*

The Nusselt number $\mathcal{N}_\infty(\sigma)$ has a broad maximum near $\sigma \simeq 4$. Thus the dependence of $\mathcal{N}$ on σ is very weak and difficult to determine from measurements with various fluids of different σ because of systematic errors due the uncertainties of the fluid properties (Ahlers & Xu 2001; Xia *et al.* 2002). We determined $\mathcal{N}(\sigma, R)$ with high precision over a narrow range of σ by using the same convection cell and by changing the mean temperature. In that case errors from different cell geometries are largely absent and the properties are known very well. Similar measurements over the ranges $5\times10^6 \leqslant R \leqslant 5\times10^8$ and $4 \leqslant \sigma \leqslant 6.5$ were made by Liu & Ecke (1997). Their results can be represented well by

$$\mathcal{N} = N_{00}\sigma^{\alpha_{eff}} R^{\gamma_{eff}} \tag{2.2}$$

with $\gamma_{eff} = 0.286$, $\alpha_{eff} = -0.030$, and $N_{00} = 0.1780$. The negative value of α_{eff} indicates that the maximum of $\mathcal{N}(\sigma)$ is below $\sigma \simeq 4$.

We used our $\Gamma = 0.67$ cell and made measurements at 30 °C, 40 °C, and 50 °C corresponding to $\sigma = 5.42$, 4.38, and 3.62 respectively. The results are included in table 3, and in the compensated form $\mathcal{N}_\infty/R^{1/3}$ they are shown as a function of R in figure 3(a). Over the range $2\times10^{10} \leqslant R \leqslant 4\times10^{11}$ they yield $\alpha_{eff} \simeq -0.044$, indicating that for this range of R also the maximum of $\mathcal{N}(\sigma)$ occurs below $\sigma = 4$. The reduced Nusselt number $\mathcal{N}_\infty\sigma^{0.044}/R^{1/3}$ is shown in figure 3(b). It shows that the data, within

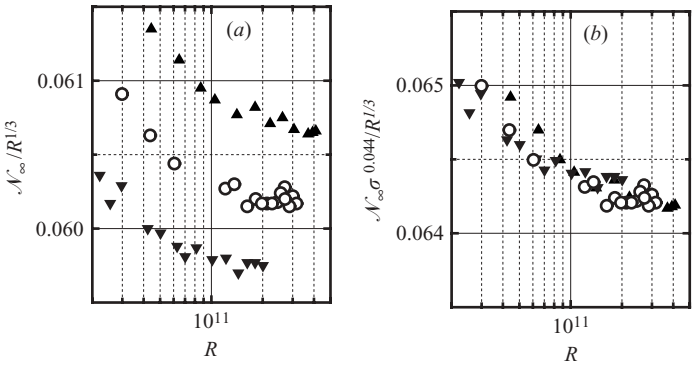

FIGURE 3. (*a*) The compensated Nusselt numbers $\mathcal{N}_\infty/R^{1/3}$ as a function of the Rayleigh number R for $\Gamma = 0.667$ at three values of the Prandtl number. (*b*) The reduced Nusselt numbers $\mathcal{N}_\infty\sigma^{0.044}/R^{1/3}$ as a function of R. Up-pointing triangles: 50 °C and $\sigma = 3.62$. Open circles: 40 °C and $\sigma = 4.38$. Down-pointing triangles: 30 °C and $\sigma = 5.42$.

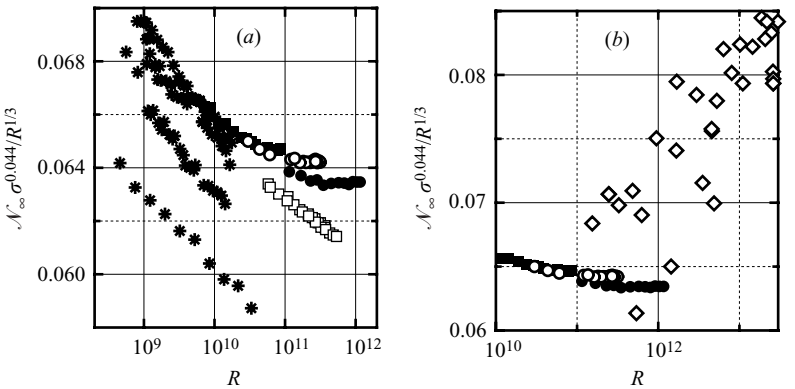

FIGURE 4. The reduced Nusselt numbers $\mathcal{N}_\infty\sigma^{0.044}/R^{1/3}$ as a function of R. (*a*) Stars: Data of Roche *et al.* (2004) for $2.5 \leqslant \sigma \leqslant 6.0$ and $\Gamma = 0.50$. Other symbols: this work for $\sigma = 4.4$ and $\Gamma = 0.98$ (solid squares), 0.67 (open circles), 0.43 (solid circles), and 0.28 (open squares). (*b*) open diamonds: data of Chavanne *et al.* (2001) for $\Gamma = 0.5$ and $2.0 \leqslant \sigma \leqslant 4.5$; solid symbols and open circles: this work for $\Gamma = 0.98$, 0.67, and 0.43.

their experimental uncertainty, collapse onto a unique curve when divided by $\sigma^{\alpha_{eff}}$. The observed σ-dependence is somewhat stronger than that of the GL model with its present parameter values.

2.4. *Comparison with other results*

Measurements of $\mathcal{N}(R)$ for $\Gamma = 0.50$ over the range $10^8 \leqslant R \leqslant 5 \times 10^{10}$ and a wide range of σ were made at cryogenic temperatures using gaseous helium by Roche *et al.* (2004). A direct, highly quantitative comparison with our results is possible only for the data points with σ-values fairly close to ours where the σ-dependence of $\mathcal{N}$ can reasonably be expected to be given by (2.2) with $\alpha_{eff} \simeq -0.044$. In figure 4(*a*) we show results of Roche *et al.* (2004) for $\mathcal{N}_\infty\sigma^{0.044}/R^{1/3}$ as a function of R. These data were corrected by the authors for the sidewall conductance, using a procedure described by them. Because of the small conductivity of helium gas one expects end-plate corrections to be negligible in this case. We also show our results for comparison. The data of Roche *et al.* (2004) fall into three well-defined groups, with

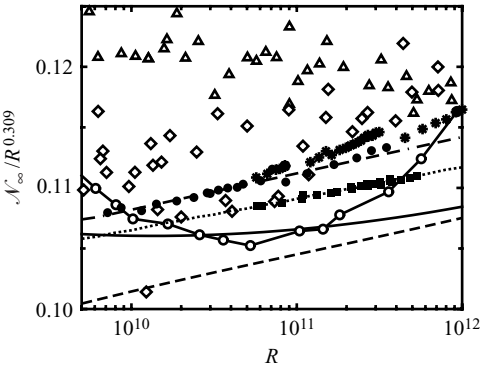

FIGURE 5. Compensated Nusselt numbers $\mathcal{N}_\infty/R^{0.309}$ as a function of R. Open circles: Niemela & Sreenivasan (2003), $\Gamma = 1, 0.7 < \sigma < 0.9$. Open triangles: Niemela *et al.* (2000), $\Gamma = 1/2, \sigma \simeq 0.7$. Open diamonds: Chavanne *et al.* (2001), $\Gamma = 1/2, 0.7 < \sigma < 2.0$. Solid circles and stars: present work, $0.43 \leqslant \Gamma \leqslant 0.98, \sigma = 4.4$. Solid squares: present work, $\mathcal{N}_\infty$, $\Gamma = 0.28, \sigma = 4.4$. Dash-dotted line: power-law fit to our data with $\Gamma \geqslant 0.43$ ($\gamma_{eff} = 0.3207$). Dotted line: power-law fit to our data for $\Gamma = 0.28$ ($\gamma_{eff} = 0.3193$). Solid (dashed) line: GL model for $\sigma = 4.4$ (0.8).

a nearly uniform vertical spacing between them of close to 4%. There is excellent agreement/consistency of the uppermost branch with our data for $\Gamma = 0.98$, 0.67, and 0.43. This is consistent with the absence of any significant aspect-ratio dependence in our data. The existence of the lower two branches is more difficult to reconcile with our results. Roche *et al.* (2004) suggest that they encountered more than one distinct state of their LSF. In our work we never found multi-stability for any Γ, and the data for $\Gamma = 0.67$ and 0.43 (which according to the calculations of Verzicco & Camussi (2003) should correspond to different flow structures) agree with each other and are consistent with the upper branch of Roche *et al.*, at least in the range where γ_{eff} has not yet saturated at $\gamma_{eff} = 1/3$. Our data for $\Gamma = 0.28$ are lower than those for our larger Γ, suggesting a difference in the LSF and indicating that the transition from a single cell to a more complicated structure occurs at $\Gamma < 0.43$ in our system. However, our results for $\Gamma = 0.28$ are only about 2% or 3% lower than the larger-Γ data and not as low as the results from the middle or lower branch of Roche *et al.*

In figure 4(*b*) we compare our results with those of Chavanne *et al.* (2001) from cryogenic experiments for $2.0 \leqslant \sigma \leqslant 4.5$ and $\Gamma = 0.50$. The end-plate corrections are expected to be negligible. Because of the low conductivity of the fluid, the sidewall contribution to the conductance of the cell is significant, but apparently no correction was made. The authors interpret their data to imply $\gamma_{eff} \simeq 0.38$, and attribute the large value to a breakdown of the boundary layers adjacent to the top and bottom plates. In that case one expects that a new regime first proposed by Kraichnan (1962) with an asymptotic exponent $\gamma = 1/2$ (and logarithmic corrections) should be entered. Our data do not reveal such a large exponent, and in the overlapping range $10^{11} \lesssim R \lesssim 2 \times 10^{12}$ remain consistent with $\gamma_{eff} = 1/3$.

Finally, in figure 5 we compare our results for $\Gamma = 0.98$, 0.67, and 0.43 (solid circles where $\gamma_{eff} \simeq 0.32$ and stars where $\gamma_{eff} \simeq 0.333$) and $\Gamma = 0.28$ (solid squares) on a less sensitive vertical scale with several measurements at cryogenic temperatures. A more comprehensive comparison was presented by Niemela & Sreenivasan (2003, referred to as NS) (we choose the same representation in terms of $\mathcal{N}_\infty/R^{0.309}$ that was used by them in their figure 5). There are systematic differences between the data sets that

are, according to NS, larger than possible systematic errors in the experiments. Our data show very little change of γ_{eff} with R, and the solid circles in figure 5 yield $\gamma_{eff} \simeq 0.321$. The data by NS (connected open circles) show a dependence on R that differs from ours, with γ_{eff} varying from about 0.28 to about 0.35 as R changes from 10^9 to 10^{12}. The data of Niemela *et al.* (2000) do not show such a strong variation of γ_{eff} and can be described well by a single $\gamma_{eff} = 0.30$ over the R-range of the figure. The data of Chavanne *et al.* (2001) (open diamonds) are on average slightly larger than ours, but over the range of R shown in the figure they have an R-dependence that is consistent with that of ours (see, however, figure 4*b*).

We have been unable to rationalize the large variations of the effective exponents of $\mathcal{N}$ from one experiment to another, and in the case of the data of NS within a single experiment with R. NS suggested that differences in the LSF structure are responsible, and state that "such differences seem to arise from delicate interplay among detailed geometry as well as Prandtl and Rayleigh numbers". Looking at our data, the absence of any significant Γ-dependence is apparent from the clustering of the data for $\Gamma \geqslant 0.43$ (solid circles) near the straight dash-dotted line corresponding to $\gamma_{eff} = 0.3207$; i.e. Γ *per se* does not play a major role. Even for $\Gamma = 0.28$, where the data are displaced vertically in the figure, presumably because of a change in the LSF, they have nearly the same effective exponent $\gamma_{eff} = 0.3193$ (dotted line). Thus it appears from our data that differences in the LSF do not have a large effect on the R-dependence of $\mathcal{N}_\infty(R)$. We wish we had a more satisfying explanation of the different results obtained by the various experiments.

This work was supported by the US Department of Energy through Grant DE-FG03-87ER13738.

REFERENCES

Ahlers, G. 2000 Effect of sidewall conductance on heat-transport measurements for turbulent Rayleigh-Benard convection. *Phys. Rev.* E **63**, 015303-1–4(R).

Ahlers, G., Grossmann, S. & Lohse, D. 2002 Hochpräzision im Kochtopf: Neues zur turbulenten Konvektion. *Z. Physik* **1** (2), 31–37.

Ahlers, G. & Xu, X. 2001 Prandtl number dependence of heat transport in turbulent Rayleigh-Bénard convection. *Phys. Rev. Lett.* **86**, 3320–3323.

Brown, E., Nicolaenko, A., Funfschilling, D. & Ahlers, G. 2005 Heat transport in turbulent Rayleigh–Bénard convection: Effect of finite top and bottom plate conductivity. *Phys. Fluids* (to be submitted).

Chaumat, S., Castaing, B. & Chillá, F. 2002 Rayleigh-Bénard cells: influence of the plates properties *Advances in Turbulence IX, Proc. Ninth European Turbulence Conference* (ed. I. P. Castro & P. E. Hancock). CIMNE, Barcelona.

Chavanne, X., Chillà, B., Chabaud, B., Castaing, B. & Hebral, B. 2001 Turbulent Rayleigh-Bénard convection in gaseous and liquid He. *Phys. Fluids* **13**, 1300–1320.

Grossmann, S. & Lohse, D. 2000 Scaling in thermal convection: a unifying view. *J. Fluid Mech.* **407**, 27–56.

Grossmann, S. & Lohse, D. 2001 Thermal convection for large Prandtl number. *Phys. Rev. Lett.* **86**, 3317–3319.

Grossmann, S. & Lohse, D. 2002 Prandtl and Rayleigh number dependence of the Reynolds number in turbulent thermal convection. *Phys. Rev.* E **66**, 016305.

Grossmann, S. & Lohse, D. 2003 On geometry effects in Rayleigh-Bénard convection. *J. Fluid Mech.* **486**, 105–114.

Grossmann, S. & Lohse, D. 2004 Fluctuations in turbulent Rayleigh-Bénard convection: the role of plumes *Phys. Fluids*, in press.

Kadanoff, L. P. 2001 Turbulent heat flow: Structures and scaling. *Phys. Today* **54** (8), 34–39.

Kraichnan, R. 1962 Turbulent thermal convection at arbitrary Prandtl number. *Phys. Fluids* **5**, 1374–1389.

Krishnamurty, R. & Howard, L. N. 1981 Large-scale flow generation in turbulent convection. *Proc. Natl Acad. Sci. USA* **78**, 1981–1985.

Liu, Y. & Ecke, R. E. 1997 Heat transport scaling in turbulent Rayleigh-Bénard convection: Effects of rotation and Prandtl number. *Phys. Rev. Lett.* **79**, 2257–2260.

Niemela, J. J., Skrbek, L., Sreenivasan, K. R. & Donnelly, R. J. 2000 Turbulent convection at very high Rayleigh numbers. *Nature* **404**, 837–840.

Niemela, J. & Sreenivasan, K. R. 2003 Confined turbulent convection. *J. Fluid Mech.* **481**, 355–384.

Roche, P., Castaing, B., Chabaud, B. & Hebral, B. 2004 Heat transport in turbulent Rayleigh-Bénard convection below the ultimate regime. *J. Low Temp. Phys.* **134**, 1011–1042.

Roche, P., Castaing, B., Chabaud, B., Hebral, B. & Sommeria, J. 2001 Side wall effects in Rayleigh-Bénard experiments. *Europhys. J.* B **24**, 405–408.

Siggia, E. D. 1994 High Rayleigh number convection. *Annu. Rev. Fluid Mech.* **26**, 137–168.

Verzicco, R. 2002 Side wall finite-conductivity effects in confined turbulent thermal convection. *J. Fluid Mech.* **473**, 201–210.

Verzicco, R. 2004 Effects of non-perfect thermal sources in turbulent thermal convection. *Phys. Fluids* **16**, 1965–1979.

Verzicco, R. & Camussi, R. 2003 Numerical experiments on strongly turbulent thermal convection in a slender cylindrical cell. *J. Fluid Mech.* **477**, 19–49.

Xia, K.-Q., Lam, S. & Zhou, S.-Q. 2002 Heat-flux measurements in high-Prandtl-number Rayleigh-Bénard convection. *Phys. Rev. Lett.* **88**, 064501.

Xu, X., Bajaj, K. M. S. & Ahlers, G. 2000 Heat transport in turbulent Rayleigh-Bénard convection. *Phys. Rev. Lett.* **84**, 4357–4360.

Wu, X.-Z. & Libchaber, A. 1992 Scaling relations in thermal turbulence – the aspect ratio dependence. *Phys. Rev.* A **45**, 842–845.